

Spin-Wave Relaxation by Eddy Currents in $\text{Y}_3\text{Fe}_5\text{O}_{12}/\text{Pt}$ Bilayers and a Way to Suppress It

Sergey A. Bunyaev,¹ Rostyslav O. Serha,² Halyna Yu. Musienko-Shmarova¹,² Alexander J.E. Kreil¹,²
Pascal Frey,² Dmytro A. Bozhko¹,^{2,3} Vitaliy I. Vasyuchka¹,² Roman V. Verba,⁴
Mikhail Kostylev,⁵ Burkard Hillebrands¹,² Gleb N. Kakazei¹,² and Alexander A. Serga¹,^{2,*}

¹*Institute of Physics for Advanced Materials, Nanotechnology and Photonics (IFIMUP), Departamento de Física e Astronomia, Universidade do Porto, Porto 4169-007, Portugal*

²*Fachbereich Physik and Landesforschungszentrum OPTIMAS, Technische Universität Kaiserslautern, Kaiserslautern 67663, Germany*

³*Department of Physics and Energy Science, University of Colorado at Colorado Springs, Colorado Springs, Colorado 80918, USA*

⁴*Institute of Magnetism, Kyiv 03142, Ukraine*

⁵*Department of Physics and Astrophysics, M013, University of Western Australia, Crawley, Washington 6009, Australia*

(Received 27 November 2019; revised 17 July 2020; accepted 27 July 2020; published 31 August 2020)

Because of their record-low intrinsic magnetic damping properties, single-crystal yttrium-iron-garnet (YIG) films serve as an excellent model medium for studying magnon-induced spintronic phenomena such as spin pumping and the spin-orbit torque effect. For this purpose, YIG films are covered with sub-skin-depth layers of nonmagnetic heavy metals with strong spin-orbit coupling. In the present work, we show experimentally and theoretically that ohmic losses of spin-wave-induced microwave eddy currents in the heavy-metal layer deliver a strong contribution to spin-wave damping in these hybrid structures. We demonstrate that this adverse effect can be controlled and largely eliminated by placing a highly conducting metal plate near to the surface of the YIG/Pt structures. These findings are of value for a proper interpretation of experiments on the magnon spintronic effects and for the design of future magnon spintronic devices.

DOI: 10.1103/PhysRevApplied.14.024094

I. INTRODUCTION

Magnonics is a field of technology that exploits spin waves (SWs) for processing information at microwave frequencies [1]. One challenge for this field is the finite lifetime of magnons (quanta of SWs) even in the lowest-damping magnetic material—single-crystal yttrium iron garnet (YIG) [2,3]. A way to tackle this problem is by compensating SW damping via transfer of a spin torque to a magnetic medium by a spin-polarized electron current, which may be generated by a dc electric current or by a thermal gradient in an adjacent nonmagnetic metal layer with strong spin-orbit interaction (Pt, Pd, Ta, etc.) [4–8]. References [9,10] report the experimental observation of a decrease in damping of spin waves propagating in YIG films capped with a Pt layer with a nanometer-range thickness in the presence of a dc current in Pt. However, the SW attenuation in those layered structures in the absence of the current appears to be a problem for practical applications.

Therefore, it is important to determine the origin of the excessive SW damping in such bilayers [11–17] and to find a way to reduce this effect.

In this work, we investigate the origin of the additional SW attenuation experimentally. We carry out measurements of standing SW resonances in a film sample with finite in-plane sizes. The measurements are performed by placing a YIG/Pt sample in a rectangular waveguide parallel and close to a metal plunger that shunts the waveguide's end (see Fig. 1). We find a peculiar behavior in the line widths of resonances of standing spin waves across the in-plane sizes of the sample as a function of the sample's distance from the plunger surface. By comparing the observed line widths with our theoretical calculations, we show that the additional SW attenuation originates from ohmic losses due to the excitation of microwave eddy currents in Pt layer by the precessing magnetization vector in YIG. The placement of a highly conducting and thick metal plate (the waveguide plunger) near the Pt layer suppresses the eddy currents in platinum [18] and thus eliminates the excessive SW damping.

*serga@physik.uni-kl.de

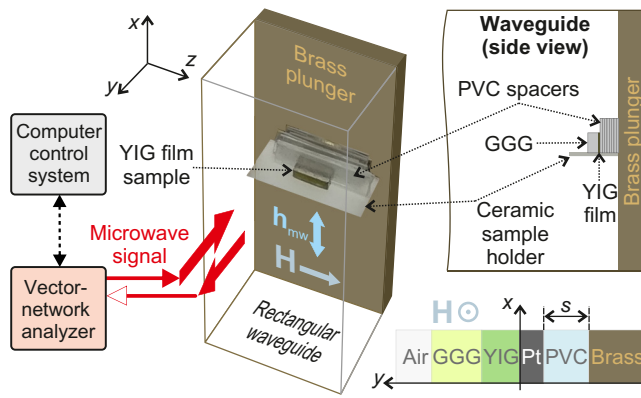


FIG. 1. The experimental setup. The figure shows a brass plunger inserted in a rectangular waveguide. The permanent magnetic field \mathbf{H} is applied along the short side of the waveguide, that is, perpendicularly to the microwave magnetic field \mathbf{h}_{mw} at the plunger wall. The rectangular sample sits near the plunger such that the long side of the in-plane magnetized YIG film is oriented along \mathbf{H} . The distance s from the YIG film to the brass wall is determined by the number of 100- μm -thick plastic PVC spacers.

II. SETUP

To carry out our experiment, we use two rectangular samples with in-plane sizes of $1.95 \times 0.85 \text{ mm}^2$, prepared from a single-side 6.7- μm -thick YIG film grown epitaxially on top of a 500- μm -thick gadolinium-gallium-garnet (GGG) substrate. One sample is capped with a sputter-deposited 10-nm-thick Pt layer. The second YIG film is left in its virgin state and is used as a reference sample. The reference and bilayer samples are characterized employing a rectangular X -band microwave waveguide (WR90) with a $22.86 \times 10.16 \text{ mm}^2$ cross section. A brass plunger terminating the waveguide is equipped with a small dielectric shelf (see Fig. 1) that supports the sample. The sample is sitting on its longer edge on the shelf, with the film plane parallel to the plunger surface and the Pt layer facing the plunger. The film surface is either in direct electric contact with the plunger or is separated from it by a number of 100- μm -thick plastic spacers. The spacers ensure that the film surface is always parallel to the plunger surface and the number of inserted spacers dictates the distance s from the Pt to the plunger. The static magnetic field $H = 2425 \text{ Oe}$ is applied parallel to the film surface and along the longer side of the rectangular YIG-film piece.

We take measurements of the microwave power absorbed by the samples using a microwave vector-network analyzer (VNA). The VNA frequency is swept across the range of 170 MHz in the vicinity of the central frequency of 8950 MHz.

III. EXPERIMENTAL RESULTS

The magnitude of the reflection coefficient $|S_{11}|$ measured as a function of the frequency is shown in Fig. 2

for two spacer thicknesses, $s = 900 \mu\text{m}$ and $s = 0$. From the figure, one sees that the spectrum represents a family of discrete peaks. We identify the peak with the largest amplitude as the fundamental standing SW mode (FM). The amplitudes of the other peaks drop with the frequency distance from the fundamental peak. As follows from Refs. [19–21], the peaks located to the right of the fundamental mode are resonances of the Damon-Eshbach- (DE) type wave—they have more nodes of the standing wave in the direction perpendicular to the direction of the applied field \mathbf{H} than along this field. Similarly, the peaks located to the left of the FM are the backward-volume-wave- (BVMSW) type resonances—they are characterized by a larger number of nodes along \mathbf{H} compared to their number in the perpendicular direction. Accordingly, the FM is characterized by the absence of nodes of the standing wave. Therefore, its wave number is close to zero. It is not perfectly zero, because of the presence of effective dipole pinning of the dynamic magnetization at the upper and lower edges of the film (Fig. 1) [22–24] and also because of the reduction in the amplitude of the dynamic magnetization at the left- and right-hand edges of the film due to the presence of a static demagnetizing field near these edges (see inset to Fig. 2 in Ref. [25]). In order to identify the observed peaks and to assign specific wave numbers to the fundamental and high-order resonances, we utilize the theory of the spectrum of traveling spin waves in a continuous magnetic film [26] and introduce in-plane wave-number quantization [19]. This approach allows us to associate the fundamental (0,0) oscillation observed at the frequency $f_{\text{FMR}} = 8950 \text{ MHz}$ with the lowest BVMSW mode.

In the following, we focus on the line width Δf_{FMR} of the fundamental mode. From Fig. 2, one sees that both the presence of the Pt layer and the dielectric spacer thickness have strong effects on Δf_{FMR} . The line width is the smallest for the reference YIG film in the presence of the PVC spacer. In this case, Δf_{FMR} , which is determined as the full line width at half maximum, is 2.61 MHz (Fig. 2). In practice, placing the bare YIG film directly on the plunger does not change Δf_{FMR} —it is now 2.65 MHz [Fig. 2(b)]. Remarkably, Δf_{FMR} for the YIG/Pt bilayer is very similar to both former cases [3.04 MHz in Fig. 2(c)] if the Pt layer is in contact with the plunger but moving the bilayer sample away from the plunger increases Δf_{FMR} by up to a factor of 3—to 9.11 MHz [Fig. 2(d)]. The dependencies of Δf_{FMR} on s for the bare and Pt-covered YIG films are the main experimental finding of our work. They are shown in Fig. 3.

IV. THEORETICAL MODEL AND CALCULATIONS

In order to explain these results, we develop a simple theory for the frequencies and damping rates of the standing SW resonances in a YIG-film resonator located in the

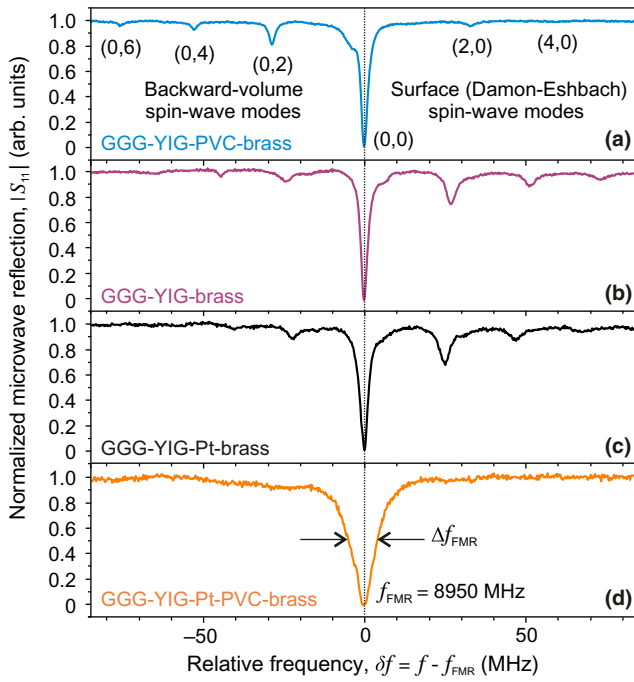


FIG. 2. Normalized SW resonance spectra of free (a),(b) YIG-film and (c),(d) YIG/Pt bilayers placed at distances $s = 0$ and $900 \mu\text{m}$ from the brass wall. The dips in the reflected power ratio S_{11} are caused by the absorption of microwave energy by SW modes excited in the rectangular YIG-film samples. These modes are standing waves with m and n nodes along the short (0.85 mm) and long (1.95 mm) sides of the YIG-film samples, respectively (and no nodes in the thickness direction). The largest dips relate to the $(m = 0, n = 0)$ mode, the frequency of which is denoted as the frequency of the ferromagnetic resonance f_{FMR} . The dips at lower frequencies correspond to $(m = 0, n = 2, 4, 6)$ modes formed by the backward-volume spin waves. The dips at higher frequencies correspond to $(m = 2, n = 0)$ and $(4, 0)$ modes formed by the surface spin waves [27]. The modes with an odd number of nodes are not excited by a homogeneous microwave magnetic field \mathbf{h}_{mw} .

vicinity of a highly conducting metallic shield. Figure 1 shows a sketch of the modeled geometry—metallic, dielectric, and ferrimagnetic layers form a stack [29] in the y direction. The layers are assumed to be continuous in the x - z plane. The bias magnetic field \mathbf{H} and the static magnetization \mathbf{M}_s for the YIG layer are parallel to the z axis. Since the sizes of the YIG sample are significantly larger than the exchange length for YIG, we neglect the exchange interaction. We solve the electrodynamic problem using Maxwell's equations and a proper magnetic permeability tensor for the ferromagnetic layer. We assume that the dynamic electric and magnetic fields for the layers have the following form:

$$h(\mathbf{r}, t), E(\mathbf{r}, t) \sim e^{-q_j y} e^{-ikz} e^{i\omega t}, \quad (1)$$

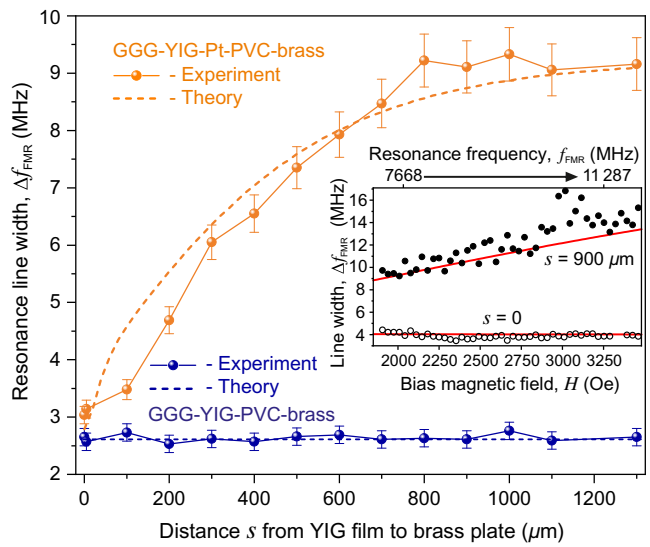


FIG. 3. The dependencies of Δf_{FMR} for the bare and platinum-covered YIG-film samples on the distance s between the YIG surface and a highly conductive metal plate. The inset shows the measured (circles) and calculated (lines) frequency dependencies of Δf_{FMR} for $s = 0$ and $900 \mu\text{m}$ [31].

i.e., we consider a BWMSV that propagates along the \mathbf{M}_s direction. In the experiment, we deal with standing-wave SW oscillations. In our model, we express the standing wave as a superposition of plane waves propagating in opposite directions. Due to the perfect reciprocity of BWMSVs, these two waves are characterized by identical dynamic field distributions and thus by equal relaxation times. Therefore, we can consider only one wave proportional to e^{ikz} with the wave number $k = \pi/d_z = 16.1 \text{ rad/cm}$, where $d_z = 1.95 \text{ mm}$ is the YIG sample size along the z direction. Nonuniformity of the SW mode profile in the x direction, which may exist due to the “effective dipole pinning” [24], is neglected (i.e., $k_x = 0$).

Substitution of Eq. (1) into Maxwell's equations yields relations between components of the electromagnetic field. A general solution for the nonmagnetic layers can be expressed as

$$\begin{aligned} h_{x,j} &= A_j e^{-q_j y} + B_j e^{q_j y}, \\ h_{z,j} &= C_j e^{-q_j y} + D_j e^{q_j y}, \\ E_{x,j} &= -\frac{i q_j}{\omega \varepsilon_j \varepsilon_0} A_j e^{-q_j y} + \frac{i q_j}{\omega \varepsilon_j \varepsilon_0} B_j e^{q_j y}, \\ E_{z,j} &= -\frac{i \omega \mu_0}{q_j} C_j e^{-q_j y} + \frac{i \omega \mu_0}{q_j} D_j e^{q_j y}, \end{aligned}$$

i.e., as a sum of independent TE and TM waves. Here, index j denotes a layer number and $q_j = \sqrt{k^2 - \omega^2 \varepsilon_j \varepsilon_0 \mu_0}$. For the conductive layers (Pt and brass), the electric permittivity is $\varepsilon = 1 - i\sigma/(\omega \varepsilon_0)$, where σ is the conductivity. The solution for the ferromagnetic layer does not separate

into TE and TM waves. It reads

$$\begin{aligned} h_x &= Ae^{-Q_1y} + Be^{Q_1y} + Ce^{-Q_2y} + De^{Q_2y}, \\ h_z &= \xi_1(Ae^{-Q_1y} - Be^{Q_1y}) + \xi_2(Ce^{-Q_2y} - De^{Q_2y}), \\ E_x &= \psi_1(Ae^{-Q_1y} + Be^{Q_1y}) + \psi_2(Ce^{-Q_2y} + De^{Q_2y}), \end{aligned}$$

$$E_z = \xi_1(Ae^{-Q_1y} - Be^{Q_1y}) + \xi_2(Ce^{-Q_2y} - De^{Q_2y}).$$

Here, $\xi_p = [\mu c^2 (Q_p^2 - k^2) + \varepsilon \omega^2 (\mu^2 - \mu_a^2)] Q_p / (k \varepsilon \mu_a \omega^2)$, $\psi_p = -i\omega \xi_p \mu_0 / Q_p$, $\zeta_p = -iQ_p / (\varepsilon \varepsilon_0 \omega)$, c is the speed of light and the “effective wave numbers” $Q_{1,2}$ are given by

$$Q_{1,2}^2 = \frac{1}{2\mu} \left[k^2(\mu + 1) - \frac{\varepsilon \omega^2}{c^2} (\mu^2 + \mu - \mu_a^2) \pm \sqrt{\left(k^2(\mu - 1) - \frac{\varepsilon \omega^2}{c^2} (\mu^2 + \mu - \mu_a^2) \right)^2 + 4 \frac{k^2 \varepsilon \mu_a^2 \omega^2}{c^2}} \right].$$

The components of the relative magnetic permeability tensor $\hat{\mu}$ for a ferromagnetic medium are given by

$$\mu = \frac{\omega_H(\omega_H + \omega_M) - \omega^2}{\omega_H^2 - \omega^2} \quad \text{and} \quad \mu_a = \frac{\omega \omega_H}{\omega_H^2 - \omega^2}, \quad (2)$$

where $\omega_H = \gamma \mu_0(H + i\Delta H)$, $\omega_M = \gamma \mu_0 M_s$, γ is the gyromagnetic ratio and ΔH is the ferromagnetic resonance line width for an isolated YIG layer (i.e., it accounts for magnetic losses only).

Using these solutions and requiring continuity of h_x , h_z , E_x , and E_z at all the boundaries, one obtains a system of 20 equation for 20 coefficients A_j , B_j , C_j , and D_j . Naturally, $B_1 = D_1 = 0$ and $A_6 = C_6 = 0$, as they describe divergent at $\pm\infty$ solutions for air and brass, respectively (see Fig. 1). The condition of compatibility (vanishing determinant) for this system of linear equations yields a relation between a complex-valued frequency and the SW wave number $\omega = \omega(k_z)$. The real part of ω represents the frequency of a standing-wave resonance, while the imaginary part is the respective resonance line width, which accounts for magnetic and electric losses in the entire structure.

In order to calculate ω , we assume the following material parameters. The brass layer and the Pt film have conductivities of 5.96×10^7 S/m and 1.3×10^6 S/m, respectively. The PVC layer has vanishing conductivity and a permittivity of 2.5. The YIG layer, GGG substrate, and semi-infinite air-filled space (denoted as “Air” in Fig. 1) are assumed to be dielectrics with zero conductivity. The permittivities of YIG and GGG are 15 [30]. Additionally, for YIG $M_s = 140$ kA/m, $\Delta H = 35.8$ A/m (i.e., 0.45 Oe), $\gamma = 2\pi \times 28$ GHz/T.

Numerical evaluation of the complex-valued eigenfrequencies for these material parameters delivers a dependence of the resonance line for the YIG/Pt bilayer sample on the distance s as shown in Fig. 3. One sees that both experiment and theory demonstrate an efficient control of the SW damping in the YIG/Pt bilayer by varying the distance s between the Pt and the brass plunger. The inset

to Fig. 3 shows that the control is possible over a broad frequency range.

One also sees that the agreement between theory and experiment is rather good despite the used approximation of $k_x = 0$. This good agreement allows us to infer that the drastic increase in the FMR line width for the YIG/Pt bilayer is due to ohmic losses of eddy currents [32–38] excited in the Pt layer in the presence of magnetization dynamics in YIG.

V. DISCUSSION

The electromagnetic boundary conditions at the surface of a thick metal plate (i.e., the thickness of which considerably exceeds the skin depth), require the direction of a microwave electric field, created by the precessing magnetization, to be close to perpendicular to the metal surface. When the very thin Pt layer sits directly on the brass plunger, the lines of the electric field cannot tilt significantly from the perpendicular at the brass surface, after crossing the 10 nm of Pt thickness. Correspondingly, the tangential component $\mathbf{E}_\tau = E_x \mathbf{e}_x + E_z \mathbf{e}_z$ of the electric field vanishes in the Pt layer as shown in Fig. 4(a). This ensures that the eddy currents induced by this field in the Pt layer are small and that most of the eddy currents circulate in brass [see Fig. 4(c) for $s \rightarrow 0$]. In this case, the ohmic losses in Pt are close to zero and the ohmic losses in brass are also rather low due to the high conductivity of brass [see Fig. 4(d) for $s \rightarrow 0$]. With an increase in s , the electric field in the plunger decouples more and more from the field in Pt due to the localized character of the electromagnetic fields generated by spin waves. This gradually relaxes the requirement for the perpendicularity of the electric field at the Pt surface facing the plunger [note a nonvanishing tangential-field value \mathbf{E}_τ in Pt in Fig. 4(b)]. This allows more efficient driving of eddy currents in Pt [see Fig. 4(c)]. Ultimately, for sufficiently large s values, the Pt layer becomes exposed to a strong oblique microwave electric field. Because the layer

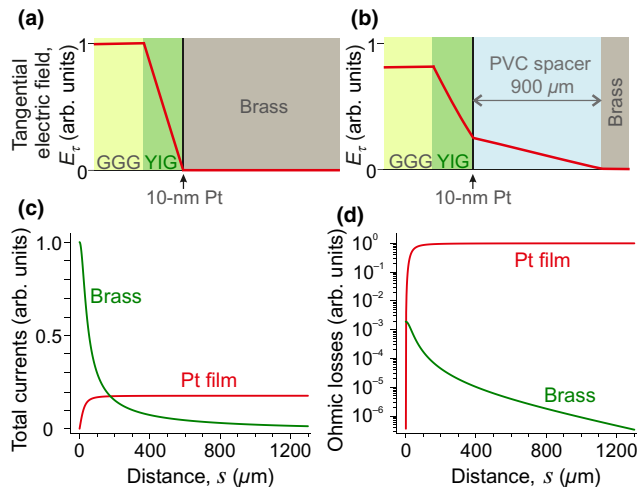


FIG. 4. The calculated profiles of the magnitude of the tangential component of the electric field E_t for two different s values: (a) $s = 0$ and (b) $s = 900$ μm. The total microwave currents in the conducting layers (c) and the corresponding ohmic losses (d), calculated for a constant amplitude of the fundamental SW mode as functions of s . The total current is calculated as the integral of the microwave current density over the thickness. The ohmic losses represent the microwave power absorbed in the respective metal layers.

thickness is much smaller than the skin depth, this situation leads to large ohmic losses for $s > 400$ μm [Fig. 4(d)] resulting in strong broadening of the SW resonances [see, e.g., Fig. 2(d)].

This model is also in good agreement with the measurements conducted for the reference YIG film without capping Pt. As seen from the same Fig. 3, no dependence of Δf_{FMR} on s is registered for this sample—in full agreement with our calculation.

In addition, we compare the eddy current and spin-pumping contributions to the total damping for YIG films of different thicknesses. The value of the spin-mixing conductance of $G_{\uparrow\downarrow} = 1.5 \times 10^{14}$ S/m² taken from Ref. [4] is used in the calculation. Our estimation shows that the eddy-current contribution decreases linearly to nearly zero values with a decrease in the YIG-film thickness from 6.7 μm to tens of nanometers. Although the contribution of spin pumping increases in thin films, for the given experimental conditions it becomes significant only for films thinner than 1 μm. For our YIG thickness, this contribution is just 0.14 MHz.

VI. CONCLUSION

In conclusion, we investigate the influence of a platinum capping layer with a thickness smaller than the skin depth on standing SW resonances in a YIG-film resonator. We find that the resonance line width depends strongly on the distance from the surface of the bilayer structure to a highly

conducting surface of a thick metal plate that is placed parallel to the structure surface. For large distances from the plate, when no impact of the plate on the magnetization dynamics is expected, the resonance line width for the bilayer structure is found to be around 3 times the line width for a reference single-layer YIG film. This behavior is in agreement with our theory, the central point of which is the inclusion of conductivities of the platinum layer and the plate in the equations. The theory explains the observed broadening of the resonance line as due to ohmic losses, of eddy currents induced in Pt by the precessing magnetization in the micrometer-thick YIG layer.

Importantly, our work shows that a strong reduction of the relaxation of magnetization precession in the heavy-metal-covered YIG-film structures can be achieved by shunting the eddy currents circulating in the heavy-metal layer with a highly conducting metal plate. For maximum effect, the thickness of the plate should exceed the skin depth for the plate material.

ACKNOWLEDGMENTS

Financial support by the Deutsche Forschungsgemeinschaft (DFG, German Research Foundation) within project B01 of the Transregional Collaborative Research Center—TRR 173—268565370 “Spin+X” is acknowledged. M.K. acknowledges his sabbatical leave from the University of Western Australia. A.A.S., V.I.V., A.J.E.K., P.F., R.O.S., and H.Yu.M.-S. acknowledge travel support from DAAD. S.A.B. and G.N.K. acknowledge the support of the Network of Extreme Conditions Laboratories—NECL and the Portuguese Foundation of Science and Technology (FCT) through Projects No. NORTE-01-0145-FEDER-022096, No. PTDC/FIS-MAC/31302/2017, and No. EXPL/IF/00541/2015. R.V.V. acknowledges support from the Ministry of Education and Science of Ukraine (Project No. 0118U004007).

- [1] A. V. Chumak, V. I. Vasyuchka, A. A. Serga, and B. Hillebrands, Magnon spintronics, *Nat. Phys.* **11**, 453 (2015).
- [2] V. Cherepanov, I. Kolokolov, and V. L'vov, The saga of YIG: Spectra, thermodynamics, interaction and relaxation of magnons in a complex magnet, *Phys. Rep.—Rev. Sec. Phys. Lett.* **229**, 81 (1993).
- [3] A. A. Serga, A. V. Chumak, and B. Hillebrands, YIG magnonics, *J. Phys. D: Appl. Phys.* **43**, 264002 (2010).
- [4] A. Hamadeh, O. d'Allivy Kelly, C. Hahn, H. Meley, R. Bernard, A. H. Molpeceres, V. V. Naletov, M. Viret, A. Anane, V. Cros, S. O. Demokritov, J. L. Prieto, M. Muñoz, G. de Loubens, and O. Klein, Full Control of the Spin-Wave Damping in a Magnetic Insulator Using Spin-Orbit Torque, *Phys. Rev. Lett.* **113**, 197203 (2014).
- [5] V. Lauer, D. A. Bozhko, T. Brächer, P. Pirro, V. I. Vasyuchka, A. A. Serga, M. B. Jungfleisch, M. Agrawal, Yu. V. Kobljanskyj, G. A. Melkov, C. Dubs, B. Hillebrands,

- and A. V. Chumak, Spin-transfer torque based damping control of parametrically excited spin waves in a magnetic insulator, *Appl. Phys. Lett.* **108**, 012402 (2016).
- [6] M. Evelt, C. Safranski, M. Aldosary, V. E. Demidov, I. Barsukov, A. P. Nosov, A. B. Rinkevich, K. Sobotkiewich, X. Li, J. Shi, I. N. Krivorotov, and S. O. Demokritov, Spin Hall-induced auto-oscillations in ultrathin YIG grown on Pt, *Sci. Rep.* **8**, 1269 (2018).
- [7] M. B. Jungfleisch, T. An, K. Ando, Y. Kajiwara, K. Uchida, V. I. Vasyuchka, A. V. Chumak, A. A. Serga, E. Saitoh, and B. Hillebrands, Heat-induced damping modification in yttrium iron garnet/platinum hetero-structures, *Appl. Phys. Lett.* **102**, 062417 (2013).
- [8] C. Safranski, I. Barsukov, H. K. Lee, T. Schneider, A. A. Jara, A. Smith, H. Chang, K. Lenz, J. Lindner, Y. Tserkovnyak, M. Wu, and I. N. Krivorotov, Spin caloritronic nano-oscillator, *Nat. Commun.* **8**, 117 (2017).
- [9] Z. Wang, Y. Sun, M. Wu, V. Tiberkevich, and A. Slavin, Control of Spin Waves in a Thin Film Ferromagnetic Insulator through Interfacial Spin Scattering, *Phys. Rev. Lett.* **107**, 146602 (2011).
- [10] E. Padrón-Hernández, A. Azevedo, and S. M. Rezende, Amplification of spin waves in yttrium iron garnet films through the spin Hall effect, *Appl. Phys. Lett.* **99**, 192511 (2011).
- [11] S. M. Rezende, R. L. Rodríguez-Suárez, M. M. Soares, L. H. Vilela-Leão, D. Ley Domínguez, and A. Azevedo, Enhanced spin pumping damping in yttrium iron garnet/Pt bilayers, *Appl. Phys. Lett.* **102**, 012402 (2013).
- [12] S. M. Rezende, R. L. Rodríguez-Suárez, and A. Azevedo, Magnetic relaxation due to spin pumping in thick ferromagnetic films in contact with normal metals, *Phys. Rev. B* **88**, 014404 (2013).
- [13] Y. Sun, H. Chang, M. Kabatek, Y.-Y. Song, Z. Wang, M. Jantz, W. Schneider, M. Wu, E. Montoya, B. Kardasz, B. Heinrich, S. G. E. te Velthuis, H. Schultheiss, and A. Hoffmann, Damping in Yttrium Iron Garnet Nanoscale Films Capped by Platinum, *Phys. Rev. Lett.* **111**, 106601 (2013).
- [14] J. Sklenar, W. Zhang, M. B. Jungfleisch, W. Jiang, H. Chang, J. E. Pearson, M. Wu, J. B. Ketterson, and A. Hoffmann, Driving and detecting ferromagnetic resonance in insulators with the spin Hall effect, *Phys. Rev. B* **92**, 174406 (2015).
- [15] D. A. Bozhko, A. A. Serga, M. Agrawal, B. Hillebrands, and M. P. Kostylev, Low-damping transmission of spin waves through YIG/Pt-based layered structures for spin-orbit-torque applications, arXiv:1603.09201 (2016).
- [16] H. Chang, P. A. P. Janantha, J. Ding, T. Liu, K. Cline, J. N. Gelfand, W. Li, M. C. Marconi, and M. Wu, Role of damping in spin Seebeck effect in yttrium iron garnet thin films, *Sci. Adv.* **3**, e1601614 (2017).
- [17] M. M. Qaid, T. Richter, A. Müller, C. Hauser, C. Ballani, and G. Schmidt, Radiation damping in ferromagnetic resonance induced by a conducting spin sink, *Phys. Rev. B* **96**, 184405 (2017).
- [18] I. S. Maksymov, Z. Zhang, C. Chang, and M. Kostylev, Strong eddy-current shielding of ferromagnetic resonance response in sub-skin-depth-thick conducting magnetic multilayers, *IEEE Magn. Lett.* **5**, 3500104 (2014).
- [19] R. Gieniusz, Cubic and uniaxial anisotropy effects on magnetostatic model in (111)-oriented yttrium iron garnet films, *J. Magn. Magn. Mater.* **119**, 187 (1993).
- [20] B. E. Storey, A. O. Tooke, A. P. Cracknell, and J. A. Przystawa, The determination of the frequencies of magnetostatic modes in rectangular thin films of ferrimagnetic yttrium iron garnet, *J. Phys. C: Solid State Phys.* **10**, 875 (1977).
- [21] R. L. White and I. H. Soit, Jr., Multiple ferromagnetic resonance in ferrite spheres, *Phys. Rev.* **104**, 56 (1956).
- [22] K. Yu. Guslienko, S. O. Demokritov, B. Hillebrands, and A. N. Slavin, Effective dipolar boundary conditions for dynamic magnetization in thin magnetic stripes, *Phys. Rev. B* **66**, 132402 (2002).
- [23] K. Yu. Guslienko and A. N. Slavin, Boundary conditions for magnetization in magnetic nanoelements, *Phys. Rev. B* **72**, 014463 (2005).
- [24] Q. Wang, B. Heinz, R. Verba, M. Kewenig, P. Pirro, M. Schneider, T. Meyer, B. Lägel, C. Dubs, T. Brächer, and A. V. Chumak, Spin Pinning and Spin-Wave Dispersion in Nanoscopic Ferromagnetic Waveguides, *Phys. Rev. Lett.* **122**, 247202 (2019).
- [25] A. V. Chumak, P. Pirro, A. A. Serga, M. P. Kostylev, R. L. Stamps, H. Schultheiss, K. Vogt, S. J. Hermsdoerfer, B. Laegel, P. A. Beck, and B. Hillebrands, Spin-wave propagation in a microstructured magnonic crystal, *Appl. Phys. Lett.* **95**, 262508 (2009).
- [26] B. A. Kalinikos, M. P. Kostylev, N. V. Kozhus', and A. N. Slavin, The dipole-exchange spin wave spectrum for anisotropic ferromagnetic films with mixed exchange boundary conditions, *J. Phys.: Cond. Matter* **2**, 9861 (1990).
- [27] When metal is in close vicinity to the surface of a ferrite film [YIG-brass case, Fig. 2(b)], the field distribution and, as a result, the dispersion curve for the surface spin wave changes significantly in comparison to a free ferrite film [YIG-PVC-brass case, Fig. 2(a)] [28]. This leads to changes in the frequencies of discrete standing-wave modes formed by the surface wave [compare Figs. 2(a) and 2(b)], as well as to changes in the efficiency of excitation of these modes by an external microwave magnetic field.
- [28] T. W. O'Keeffe and R. W. Patterson, Magnetostatic surface-wave propagation in finite samples, *J. Appl. Phys.* **49**, 4886 (1978).
- [29] M. Kostylev and A. A. Stashkevich, Proposal for a microwave photon to optical photon converter based on traveling magnons in thin magnetic films, *J. Magn. Magn. Mater.* **484**, 329 (2019).
- [30] S. Chen and M. N. Afsar, Fabry-Pérot open resonator technique for dielectric permittivity and loss tangent measurements of yttrium iron garnet, *IEEE Trans. Magn.* **43**, 2734 (2007).
- [31] The frequency dependencies are measured for smaller pieces cut from the same bilayer YIG-Pt film. For smaller in-plane sample sizes, a larger contribution of the process of two-magnon scattering from the sample edges to the total spin-wave attenuation is expected. This is seen as some extra broadening of the FMR line in the displayed data. The predominance of the two-magnon scattering over the Hilbert damping mechanisms in low-loss YIG films [39] also leads to a lack of frequency dependency of the FMR line width for $s = 0$.

- [32] R. E. De Wames and T. Wolfram, Characteristics of magnetostatic surface waves for a metalized ferrite slab, *J. Appl. Phys.* **41**, 5243 (1970).
- [33] N. Chan, V. Kamberský, and D. Fraitová, Impedance matrix of thin metallic ferromagnetic films and SSWR in parallel configuration, *J. Magn. Magn. Mater.* **214**, 93 (2000).
- [34] I. S. Maksymov and M. Kostylev, Broadband stripline ferromagnetic resonance spectroscopy of ferromagnetic films, multilayers and nanostructures, *Phys. E* **69**, 253 (2015).
- [35] M. Kostylev, Strong asymmetry of microwave absorption by bilayer conducting ferromagnetic films in the microstripline based broadband ferromagnetic resonance, *J. Appl. Phys.* **106**, 043903 (2009).
- [36] M. Bailleul, Shielding of the electromagnetic field of a coplanar waveguide by a metal film: Implications for broadband ferromagnetic resonance measurements, *Appl. Phys. Lett.* **103**, 192405 (2013).
- [37] H. Głowiński, M. Schmidt, I. Gościańska, J.-Ph. Ansermet, and J. Dubowik, Coplanar waveguide based ferromagnetic resonance in ultrathin film magnetic nanostructures: Impact of conducting layers, *J. Appl. Phys.* **116**, 053901 (2014).
- [38] V. Flovik, B. H. Pettersen, and E. Wahlström, Eddy-current effects on ferromagnetic resonance: Spin wave excitations and microwave screening effects, *J. Appl. Phys.* **119**, 163903 (2016).
- [39] A. V. Chumak, A. A. Serga, and B. Hillebrands, Magnonic crystals for data processing, *J. Phys. D: Appl. Phys.* **50**, 244001 (2017).